Top quarks objects definition and performance at ATLAS

V. Boisvert on behalf of the ATLAS Collaboration
Royal Holloway University of London, Egham, Surrey, TW20 0EX, UK
E-mail: veronique.boisvert@cern.ch

Abstract. The definition and performance of objects in events containing top quarks are presented. More specifically, the trigger, reconstruction and identification criteria for electrons, muons and taus are described. The selection and data calibration of jets and b-jets are also discussed. The effect of pile-up are described for each object.

1. Introduction

Top quark events contain almost the full list of objects that the ATLAS detector is capable of detecting. Since the top quark decays into a W boson and a b quark, the final state may contain electrons, muons or tau leptons from the W decay, associated with some missing transverse energy assigned to the corresponding neutrino. The W boson might also decay to a pair of quarks, which will hadronize into jets. Finally, top quark events also contain b-jets. In this note, each object definition and performance is described for the analyses that used the 7 TeV dataset of 2011 as well as the beginning of the 8 TeV dataset of 2012. The definition and performance of boosted objects in top quark events is described elsewhere in these proceedings [1].

As the instantaneous luminosity increased over time, the amount of pile-up also increased in the data, as illustrated in Fig. 1. There are two categories of pile-up: the in-time pile-up refers to multiple interactions within the same bunch crossing, while the out-of-time pile-up is associated with the fact that even though the bunch spacing in the LHC is 50 ns, some detectors collect signal for a longer time period, for example in the Liquid Argon calorimeters the drift time of the signal is between 250 and 600 ns. The pile-up present in events affects the reconstruction and performance of essentially every object in ATLAS. To mitigate the effect of pile-up, new variables have been used which preserve the object performance. For example, jet identification now requires that jets satisfy a certain amount of jet vertex fraction, defined as the fraction of track p_T associated to the jet coming from the hard scattering interaction. More details on the impact of pile-up is given in each following section.

2. Electrons

The trigger efficiency turn-on curve as a function of the electron E_T is shown in Fig. 2 [2]. The event filter electron E_T threshold varied between 20 GeV and 22 GeV over the 7 TeV dataset, while the analyses offline requirement is typically $E_T > 25$ GeV. In addition, to counter the effects of pile-up, the trigger also requests at Level 1 an upper threshold on hadronic leakage. The electron reconstruction algorithm first uses a sliding window algorithm with each electromagnetic

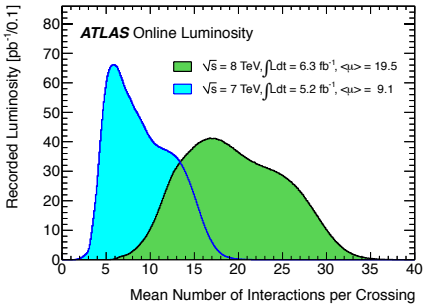

Figure 1. Mean number of interactions per crossings in the 7 TeV and 8 Tev datasets.

cluster, then it matches tracks to those clusters. Conversion photons are kept in the list to ensure high efficiency. The acceptance for electrons is defined by requesting that $|\eta_{cluster}| < 2.47$. The identification of electrons relies on a multi-variate analysis which contains various calorimeter variables. Examples of variables used for the track quality requirements include: the number of hits in the various detectors, the distance of closest approach d_0 to the primary vertex and the ratio of the number of transition radiation hits over the total number of hits on the track. At the identification stage a conversion veto is applied.

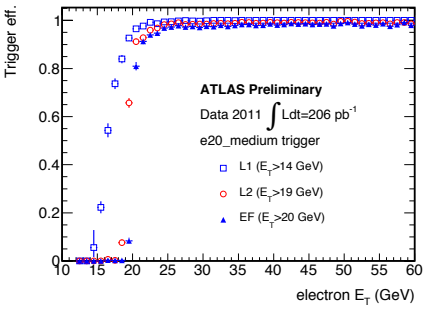

Figure 2. Trigger efficiency curve as a function of electron E_T in the 7 TeV dataset [2].

Since the electron comes from a W decay it is isolated from tracks or calorimeter clusters. The variables used to ensure that the electron is isolated are the sum of transverse energy (momentum) within a cone of ΔR[1]< 0.2 (0.3) around the electron. Instead of having a fixed cut value, the cut values are different according to the electron p_T and η in order to keep the efficiency constant at 90%.

Improvements included in the reconstruction algorithms processing the 8 TeV dataset include taking into account Bremssthralung in the track pattern recognition and the use of a Gaussian Sum Filter to refit the track associated to electromagnetic clusters. The reoptimization of the identification criteria due to the additional amount of pile-up include relaxing variables that are sensitive to pile-up, like the fraction of energy leaking into the hadronic calorimeter, while tightening other variables that are more pile-up robust, like the lateral shower shape in the first sampling [3]. The efficiency improvement due to these changes are shown in Fig 3 comparing the 7 TeV and 8 TeV dataset efficiency as a function of the electron E_T and η [4].

The calibration of the electron efficiency as well as the energy scale and resolution is obtained from data samples, using the so-called Tag and Probe method, based on testing the algorithm on the decayed objects of standard candles for electrons like J/Ψ, Z and W events [5] [6]. The systematic uncertainty on the efficiency calibration is about 2.5% (of which about 1% is from

[1] $\Delta R = \sqrt{(\Delta\phi)^2 + (\Delta\eta)^2}$

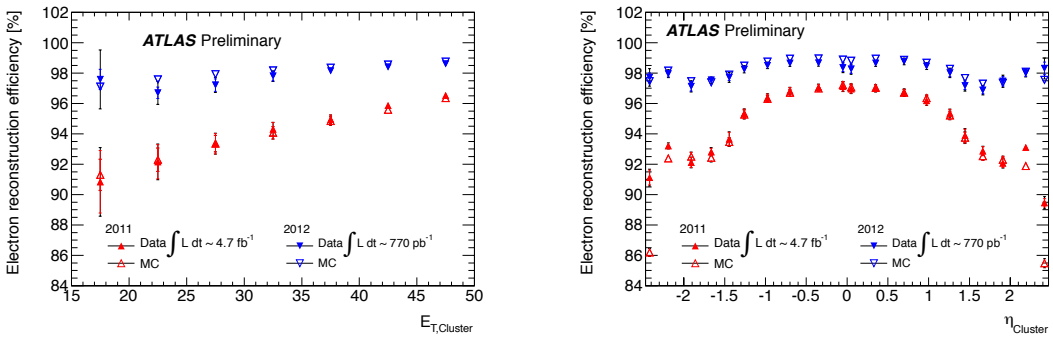

Figure 3. Electron reconstruction efficiency as a function of the electron E_T (left) and cluster η (right) showing the improvements between the 7 TeV and 8 TeV dataset [4].

the pile-up effect), while the systematic uncertainty on the energy scale and resolution is about 1.5%.

3. Muons

Shown in Fig. 4 is the muon trigger efficiency as a function of muon p_T for the 7 TeV dataset and 8 TeV dataset [7] [8]. The p_T threshold was kept at 18 GeV during the full period. Muon tracks are fit separately in the inner detector and muon spectrometer, and top quark analyses use combined tracks for muon objects. The acceptance for muons is $|\eta| < 2.5$.

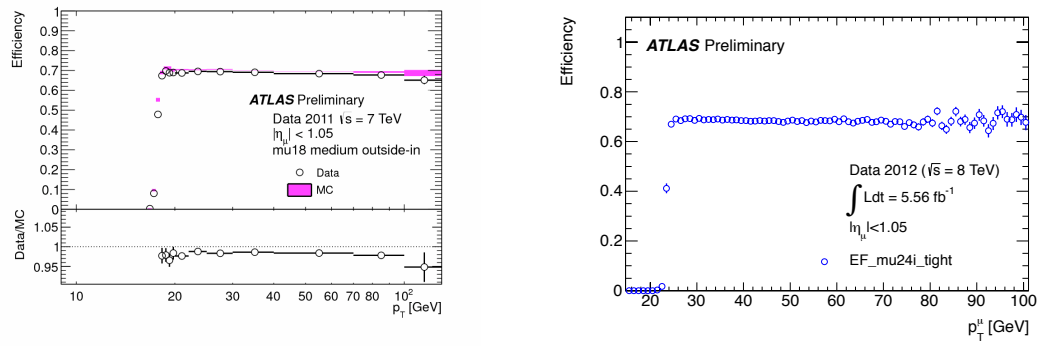

Figure 4. Muon trigger efficiency curves for the 7 TeV (left) [7] and 8 TeV (right) [8] dataset.

The isolation criteria for the muons were optimised for low dependence on pile-up and high multijet background rejection. They consist of requiring the E_T sum inside a cone of ΔR <0.2 around the muon direction to be less than 4 GeV and the p_T sum inside a cone of ΔR <0.3 to be less than 2.5 GeV. Since E_T is very affected by pile-up, it is best to require a small cone size and a large value, as opposed to p_T which is less affected by pile-up such that it is then best to require a larger cone size and a small cut value [9]. These improvements are shown in Fig. 5. As for the requirement that the muon must be a distance $\Delta R > 0.4$ from an identified jet, it is not affected by pile-up if the jet p_T >25 GeV and the jet vertex fraction is greater than 0.75. The calibration methods to determine the efficiency and resolution of muons are discussed in [10] and [11] respectively.

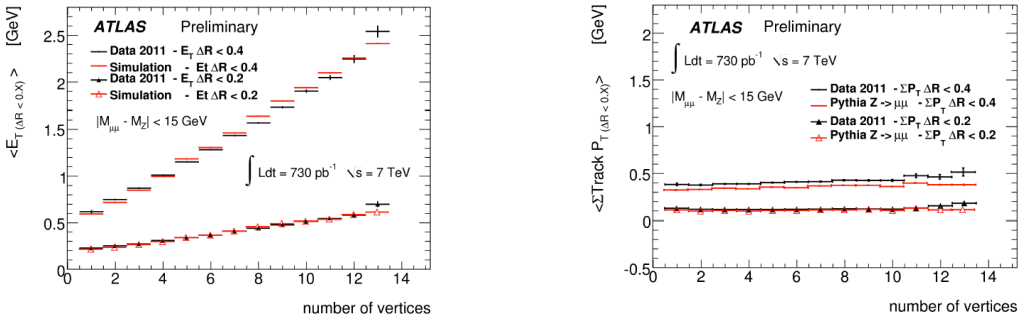

Figure 5. Comparison of different cone sizes for E_T (left) and p_T (right) showing the performance of these variables with pile-up [9].

4. Taus

The ATLAS measurement of the top quark production cross-section using taus is described in these proceedings [12]. The ATLAS reconstruction of hadronic taus is seeded by jets associated with one or greater or equal to three tracks. Various discriminants are used to remove jet and electron fakes. The jet rejection factor is about 300 for a 35% signal efficiency while the electron rejection factor is between 100 and 1000 for a 50% signal efficiency [13].

5. Jets

Reconstruction of jets relies on the anti-k_t algorithm with R=0.4 starting from topological clusters at the electromagnetic scale. A pile-up subtraction scheme at the electromagnetic scale is applied and those corrections depend on the number of primary vertices in the event, the number of primary interactions (μ) and η. Most top quark analyses require a jet vertex fraction for the jet to be greater than 0.75. The improvement provided by this requirement is shown in Fig. 6 [14].

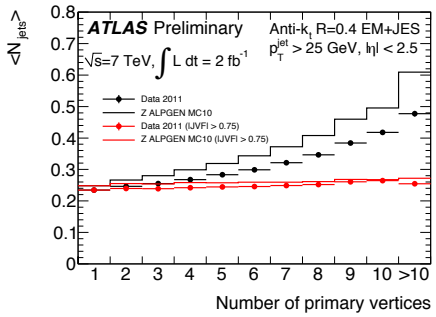

Figure 6. Average number of selected jets as a function of number of primary vertices showing the impact of requiring the jets to have a jet vertex fraction greater than 0.75 [14].

The calibration of the jet energy scale relies on Z+jets and γ+jets p_T balance for $|\eta| < 1.2$ while dijet p_T balance is used for $|\eta| > 1.2$. The jet energy scale correction factors are obtained from the full 2011 dataset and now allow for the various uncertainty sources to be nuisance parameters. Additional nuisance parameters take into account high p_T extrapolation, inter calibration for jets with high η and pile-up. The jet energy scales are expressed in such a way as to allow analyses to fit for them *in-situ*. Top quark analyses also apply uncertainties associated with: b-jets, light quark and gluon composition and close-by jet. The jet energy scale uncertainty using the Z+jets events is shown in Fig. 7 [15].

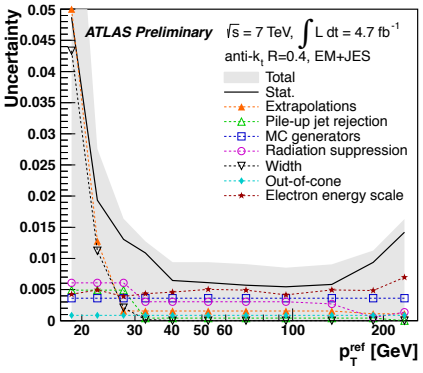

Figure 7. Jet energy scale uncertainty as a function of jet p_T using Z+jets events [15].

The jet energy resolution agrees between data and MC in both the dijet balance and bi-sector technique, such that no MC smearing is needed. There is however a systematic uncertainty on the jet energy resolution based on the uncertainty of the calibration [16].

6. b-jets

Since every top quark decays to a W and a b jets, b-jet tagging is crucial to top quark physics. The current most performant b-tagging algorithm (called MV1) is based on three tagging algorithms fed into a neural network parameterized in terms of jet p_T and η [17]. The first algorithm (JetFitterCombNN) exploits the topology of b and c hadron decays inside the jet using Kalman filtering, the likelihood uses vertex mass, momentum, flight-length significance and track multiplicity. The second algorithm (IP3D+SV1) uses the impact parameters significance as well as the z_0 significance as a reference pdf for b-jets and light-jets in the MC. Finally the third algorithm (SV0) searches for two-track vertices, and also uses the invariant mass of the tracks, the ratio of the track energy over the jet energy and the number of two-track vertices. The light jet rejection as a function of b-jet efficiency is shown in Fig. 8 for the various b-tagging algorithms [18]. The operating point used for most 7 TeV top quark analyses is at 70% efficiency.

The JetFitterCombNNc algorithm has been optimised for charm rejection to help with for example suppressing the W+c background in single top analyses. The performance of this algorithm is also shown in Fig. 8. There is also a Soft Muon Tagging algorithm which relies on a good muon inside a jet, also allowing for charge tagging of the jet.

The b-tagging efficiency scale factors between data and MC are obtained from various data-driven methods including: System 8 [19], p_T^{rel} [18] and D^* selection [20]. The methods produce compatible results, the combined calibration reduces the uncertainty, which is down below 10% and shown in Fig. 9 for the 70% operating point. Top quark events can also be used as a calibration method for b-tagging algorithms (not used in top quark analyses). The top anti-top quark calibration in the lepton+jets channel is also shown in Fig. 9. Dedicated c-jet efficiency scale factors are obtained from a dedicated D^* analysis, while for tau-jets the c-jets scale factors are used with increased uncertainty.

The probability of light jets being b-tagged is calibrated using two methods: the SV0-mass method relies on templates from MC of the invariant mass of the secondary vertex and is fit to the data, the second method is the negative tag rate method. The scale factors for efficiency and mistag rate are binned in p_T and η of the jet. Each individual systematic uncertainty is varied as well as bin-to-bin covariance matrices used. The scale factor uncertainties vary from 18% to 49% [22].

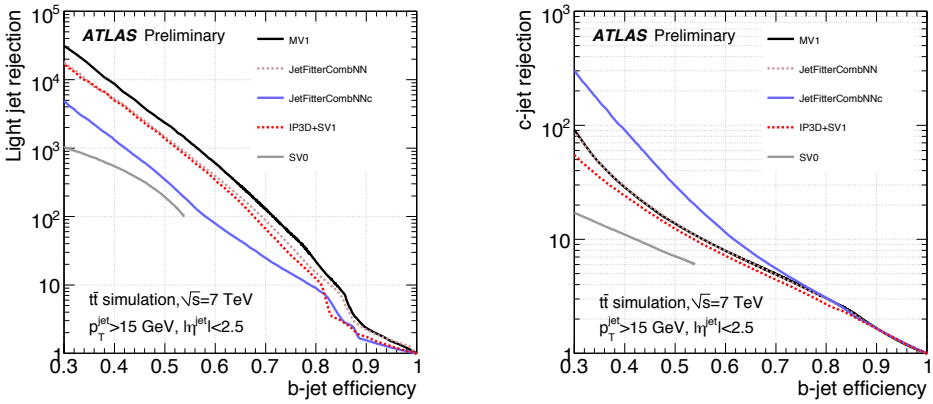

Figure 8. Comparison of the performance of various b-tagging algorithms, on the left is the light jet rejection as a function of b-jet tagging efficiency and on the right is the charm-jet rejection as a function of b-jet tagging efficiency. For most top quark analyses, the operating point is 70% b-jet tagging efficiency [18].

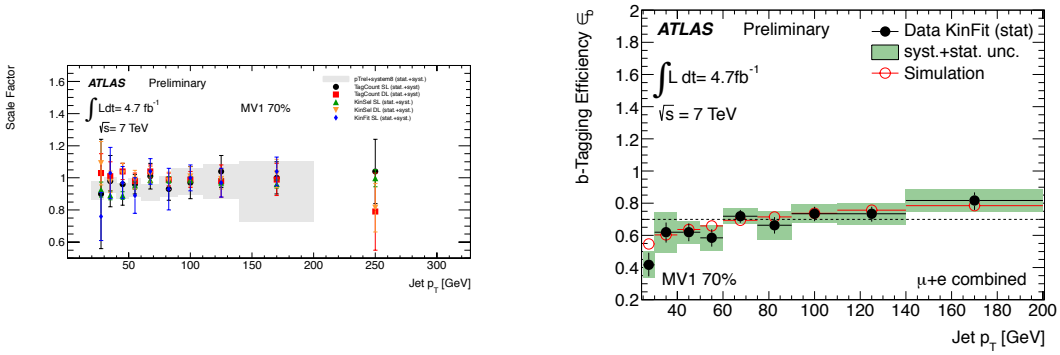

Figure 9. Left: b-jet tagging scale factors as a function of jet p_T for the different data calibration methods. Right: b-jet tagging efficiency as a function of jet p_T using the top anti-top quark events in the lepton+jets channel calibration method [21].

7. Missing Transverse Energy

The definition of missing transverse energy (E_T^{miss}), characteristic of for example the presence of a neutrino, is given by:

$$-E_{x,y}^{miss} = E_{x,y}^{RefElec} + E_{x,y}^{RefJet} + E_{x,y}^{RefSoftJet} + E_{x,y}^{RefMuon} + E_{x,y}^{CellOut}.$$

The E_T^{miss} used in top quark analyses uses top quark object definitions so that calorimeter cells are calibrated according to which objects they are associated with. Remaining energy cells are included as a CellOut term calibrated at the EM scale. Jets with $p_T > 20$ GeV are included at EM+JES scale while jets with 7 GeV $< p_T <$ 20 GeV at EM scale. The muon term uses the muon p_T of all isolated muons. Finally, the effect of pile-up will enter through the SoftJet and CellOut terms, they are a small fraction of the whole E_T^{miss} and 6.6% of the uncertainty on E_T^{miss} comes from the soft terms [23].

8. Conclusions

The ATLAS top quark object definitions and calibrations have evolved quite a lot over the 2011 7 TeV dataset. Top quark members are at the forefront of ATLAS on those topics, since top quark events involve the majority of ATLAS objects. A common thread is that a combination of methods typically offer the best performance. In some cases, the systematic uncertainty determination is quite sophisticated. Finally, the increasing amount of pile-up in the data has been a challenge but ATLAS has managed to rise to it.

References

[1] S. Fleischmann on behalf of the ATLAS and CMS collaborations, Boosted top quark techniques and searches for ttbar resonances at the LHC, *TOP 2012 Proceedings*
[2] ATLAS Collaboration, ATL-COM-DAQ-2011-032, *url: https://cds.cern.ch/record/1351827/*
[3] ATLAS Collaboration, ATL-COM-PHYS-2012-260, *url: https://cds.cern.ch/record/1430634/*
[4] ATLAS Collaboration, ATL-COM-PHYS-2012-783, *url: https://cds.cern.ch/record/1454809/*
[5] ATLAS Collaboration, ATL-COM-PHYS-2011-1637, *url: https://cds.cern.ch/record/1403075/*
[6] ATLAS Collaboration, ATL-COM-PHYS-2012-259, *url: https://cds.cern.ch/record/1430632/*
[7] ATLAS Collaboration, ATLAS-CONF-2012-099, *url: https://cds.cern.ch/record/1462601/*
[8] ATLAS Collaboration, *url: https://twiki.cern.ch/twiki/bin/view/AtlasPublic/MuonTriggerPublicResults#Muon_trigger_performances_in_201*
[9] ATLAS Collaboration, ATL-COM-PHYS-2011-1503, *url: https://cds.cern.ch/record/1395476/*
[10] ATLAS Collaboration, ATL-COM-PHYS-2011-1640, *url: https://cds.cern.ch/record/1403080/*
[11] ATLAS Collaboration, ATL-COM-PHYS-2011-1504, *url: https://cds.cern.ch/record/1395478/*
[12] G. Khoriauli on behalf of the ATLAS and CMS Collaborations, Top pair cross-section results at LHC in final states with taus or no leptons, *TOP 2012 Proceedings*
[13] ATLAS Collaboration, ATLAS-CONF-2011-152, *url: https://cds.cern.ch/record/1398195/*
[14] ATLAS Collaboration, *url: https://twiki.cern.ch/twiki/bin/view/AtlasPublic/JetEtmissApproved2011PileupOffsetAndJVF*
[15] ATLAS Collaboration, ATLAS-CONF-2012-053, *url: https://cds.cern.ch/record/1452641/*
[16] ATLAS Collaboration, *url: https://twiki.cern.ch/twiki/bin/view/AtlasPublic/JetEtmissApproved2011JetResolution*
[17] ATLAS Collaboration, ATLAS-CONF-2011-102, *url: https://cds.cern.ch/record/1369219/*
[18] ATLAS Collaboration, ATLAS-CONF-2012-043, *url: https://cds.cern.ch/record/1435197/*
[19] ATLAS Collaboration, ATLAS-CONF-2011-143, *url: https://cds.cern.ch/record/1386703/*
[20] ATLAS Collaboration, ATLAS-CONF-2012-039, *url: https://cds.cern.ch/record/1435193/*
[21] ATLAS Collaboration, ATLAS-CONF-2012-097, *url: https://cds.cern.ch/record/1460443/*
[22] ATLAS Collaboration, ATLAS-CONF-2012-040, *url: https://cds.cern.ch/record/1435194/*
[23] ATLAS Collaboration, ATLAS-CONF-2012-101, *url: https://cds.cern.ch/record/1463915/*